https://doi.org/10.5194/egusphere-2025-1059
Preprint. Discussion started: 12 May 2025

Unveiling Sulfate Aerosol Persistence as the Dominant Control of the Systematic Cooling Bias in CMIP6 Models: Quantification and Corrective Strategies

Jie Zhang[1,2*], Kalli Furtado[3*], Steven T. Turnock[4,5], Yixiong Lu[1,2], Tongwen Wu[1,2], Fang Zhang[1,2], Xiaoge Xin[1,2]

1. *State Key Laboratory of Disaster Weather Science and Technology, CMA EMPC*
2. *CMA Earth System Modeling and Prediction Centre, China Meteorological Administration, Beijing, China*
3. *Centre for climate research Singapore, Singapore*
4. *Met Office Hadley Centre, Exeter, UK*
5. *University of Leeds Met Office Strategic (LUMOS) Research Group, University of Leeds, Leeds, UK*

Corresponding to: Jie ZHANG (jiezhang@cma.gov.cn) & Kalli Furtado (Kalli_FURTADO@nea.gov.sg)

Abstract

Including sophisticated aerosol schemes in the models of the sixth Coupled Model Inter-comparison Project (CMIP6) has not improved historical climate simulations. In particular, the models underestimate the surface air temperature anomaly (SATa) when anthropogenic sulfur emissions increased in 1960~1990, making the reliability of the CMIP6 projections questionable. Biases in cooling among the models are correlated with sulfate burden and the deposition of sulfur is the process responsible. We show that the lifetime of atmospheric sulfur, defined by a new global index for sulfur deposition (an "Effective Sulfur Retention Timescale" (ESRT)), determines the cooling biases. Reducing the biases to within the observational uncertainty is consistent with a physically plausible ESRT of around one day, whereas the CMIP6 models overestimate this timescale. Based on targeting a reduction of ESRT, post-CMIP6 improvements to two models are shown to greatly improve SATa reproduction.

https://doi.org/10.5194/egusphere-2025-1059
Preprint. Discussion started: 12 May 2025

1. Introduction

Atmospheric aerosols have rapidly increased since the Industrial Revolution. Over this time period, the total aerosol effective radiative forcing (ERF) was dominated by the sulfate cooling effect, and offset a substantial portion of global-mean forcing from well-mixed greenhouse gases (IPCC, 2023). Without this historical aerosol ERF, the Paris Agreement's target of limiting global warming to 1.5ºC above pre-industrial levels would have already been missed in 2015 (Hienola et al., 2018). Similarly, stopping all present-day anthropogenic aerosol emissions is estimated to induce a global-mean surface heating of 0.5~1.1ºC (Samset et al., 2018). The year 2024 has been confirmed as the hottest year in human history, and was the first year to breach the 1.5ºC warming limit (Bevacqua et al., 2025). Moreover, recent years have seen temperature trends accelerate, which may be due to reductions in atmospheric aerosols, especially aerosols produced by commercial shipping (Hansen et al., 2025). Hence, it has been suggested that even small emissions in relatively pristine air have substantial effects, and better constraining the ability of global-climate models to predict aerosol effects may be crucial to obtaining reliable projections.

The observed temporal evolution of historical surface air temperature (SAT) is one of the major metrics used for evaluating the performance of climate models. However, the SAT anomalies in the CMIP6 models are systematically lower than was observed for the 1960~1990 period, whereas the CMIP5 models on average track the instrumental record quite well (e.g., Flynn and Mauritsen, 2020). The 1960~1990 period is referred to as the "pothole cooling period" (PHC) in our previous study (Zhang et al., 2021a), due to the 'pot-hole' shaped dip in SAT at that time, and in this study hereafter. The PHC period is coincident with the so-called Great Acceleration period, in which the human enterprise was boosted remarkably and led to global-scale impacts on Earth System functioning (Steffen et al., 2007). Recent studies hypothesized that aerosol forcing in CMIP6 is stronger than in CMIP5 and is responsible for the suppressed late 20th-century warming (Dittus et al., 2020; Smith and Forster, 2021) .

The anomalous cooling points towards a problem with the sulfur cycle in recent

https://doi.org/10.5194/egusphere-2025-1059
Preprint. Discussion started: 12 May 2025

ESMs or the emissions data (Hardacre et al., 2021; Wang et al., 2021). Considering the importance of the sulfur cycle in historical aerosol ERF, we examine the sulfur related processes in eleven CMIP6 models with aerosol schemes in this study. All the models are forced with CMIP6 historical anthropogenic aerosol emissions (Hoesly et al., 2018), and therefore differences in their sulfate burdens are mainly due to different representations of the sulfur cycle in the models.

We will identify the key processes that determine sulfate-burden in these models, and introduce a simple metric for measuring the level of activity in the sulfur cycle in the models on the global scale. This metric (an effective timescale for global cycling of atmospheric sulfate) can be easily calculated from time series of global means only, without the need for complex diagnostics of the sulfur-cycle processes. We show that our timescale is strongly correlated with sulfate burden and anomalous cooling and has a clear physical interpretation that allows each model's sulfur cycle to be calibrated using historical temperature biases.

2. Results

2.1 SAT and sulfate burden

The historical evolutions of near-global mean (60ºS to 65ºN) SATa in the eleven CMIP6 models with interactive aerosol schemes are shown in Fig. 1a. All the models tend to underestimate SATa since the 1950s. The cooling bias is most pronounced from 1960 to 1990, i.e., the PHC period. The SATa in PHC is about 0.34ºC in the observations. However, the multi-model mean (MMM) SATa in the models is about 0.3ºC lower with a large model spread. The SATa ranges from -0.24ºC in EC-Earth3-AerChem to 0.19ºC in GFDL-ESM4 and MIROC6. The cooling is noticeable at the mid to high latitude in the Northern Hemisphere (NH, as shown in the attached SATa map in Fig.1a). The sudden drop in SATa in the early 1960s and 1990s may be due to the stronger model responses to large volcanic eruptions, Mount Agung in 1963 and Mount Pinatubo in 1991, than in the observations (Chylek et al., 2020). The anomalous

https://doi.org/10.5194/egusphere-2025-1059
Preprint. Discussion started: 12 May 2025

cooling biases gets smaller later in the simulations, which is related to the generally high sensitivity of the models to GHG forcing (Smith and Forster, 2021).

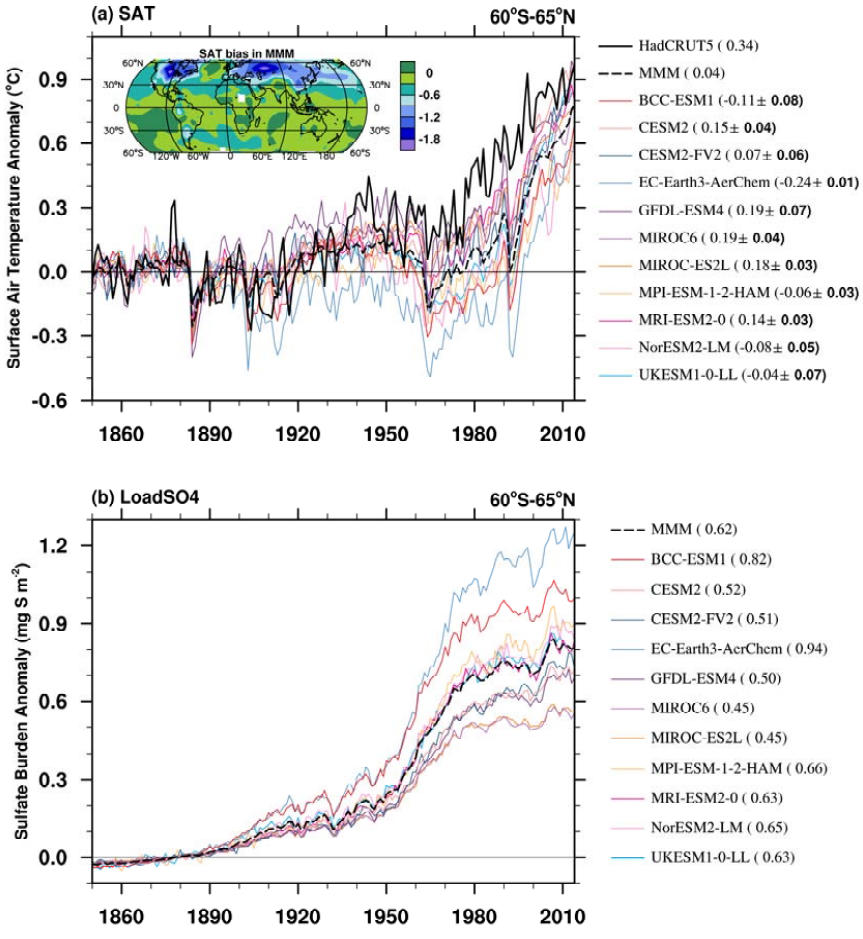

Figure 1. (a) Historical surface air temperature anomalies (SATa) relative to 1850~1900 mean for HadCRUT5 (thick black line), the ensemble mean for each CMIP6 model (solid color lines), and multi-model mean (MMM, dashed black line). The numbers in brackets are the mean results during the pothole period (1960~1990) together with the inter-member spread for each model. Panel (b) is the same as panel (a) but for sulfate burden anomalies for the first realization from each CMIP6 model (solid color lines) and MMM (dashed black line).

Global emissions of SO_2 grew steadily after the 1950s and peaked in the 1970s at

https://doi.org/10.5194/egusphere-2025-1059
Preprint. Discussion started: 12 May 2025

180Tg yr^{-1}, which is about 3.6 times the 1950s' emissions (Hoesly et al., 2018). As the main precursor of sulfate, the growing emission of SO_2 led to the accumulation of sulfate in the atmosphere, which interrupted a decades-long warming trend via the cooling effects of sulfate aerosols on climate, even though carbon-dioxide emissions continued to rise (Wilcox et al., 2013). Because of the emission control policies in Europe and North America (Hand et al., 2012; Vestreng et al., 2007), such as the Gothenburg Protocol (Eb, 1999) and the 1990 Clean Air Act Amendments in the U.S. (Likens et al., 2001), global anthropogenic SO_2 emissions were suppressed after the 1980s and SAT started to increase rapidly in the observations (Aas et al., 2019). However, anthropogenic SO_2 emission continued to increase over Asia due to industrial developments, although they have also decreased since 2006 in East Asia (Wang et al., 2021). Some of this decrease in SO_2 emissions at the beginning of the 21st century is not well represented in the CMIP6 emission inventory. But it is outside of the PHC period and the impact on SAT reproduction is beyond the scope of this paper.

In the 11 CMIP6 models, sulfate concentrations increased rapidly during the PHC period (Fig.1b). The intensified emission of anthropogenic SO_2 mainly comes from industries and the energy-transformation sector (e.g., Ohara et al., 2007; Vestreng et al., 2007). The SAT anomalies simulated by CMIP6 models are systematically lower than observations during the PHC period, indicating an excessively strong sulfate-induced cooling effect in CMIP6 models. The sulfate burden is the lowest in MIROC models (0.45 mg S m^{-2}) with the smallest cooling bias（-0.15ºC lower than HadCRUT5), and is doubled in EC-Earth3-AerChem (0.94mg S m^{-2}) with the largest cooling (-0.58ºC lower than HadCRUT5). Generally, the models with higher sulfate burdens anomalies also tend to underestimate SAT anomalies the most. As shown in Fig. 2a, the correlation coefficient between anomalous sulfate burden and SAT during the PHC is -0.91, significant at the 1% level using a Student's *t*-test. Interactive chemistry may have an impact on sulfate formation and affect the sulfate aerosol burdens in the atmosphere (Mulcahy et al., 2020). As shown in Fig.2a, models with interactive chemistry (color dots) seem to have higher sulfate burden anomaly and lower SATa than models without

https://doi.org/10.5194/egusphere-2025-1059
Preprint. Discussion started: 12 May 2025

(color circles). However, the relationship between sulfate burden and SATa is consistent among models with and without interactive chemistry (i.e., there is no obvious difference in relationship between loadSO4 and SATa for models with and without interactive chemistry).

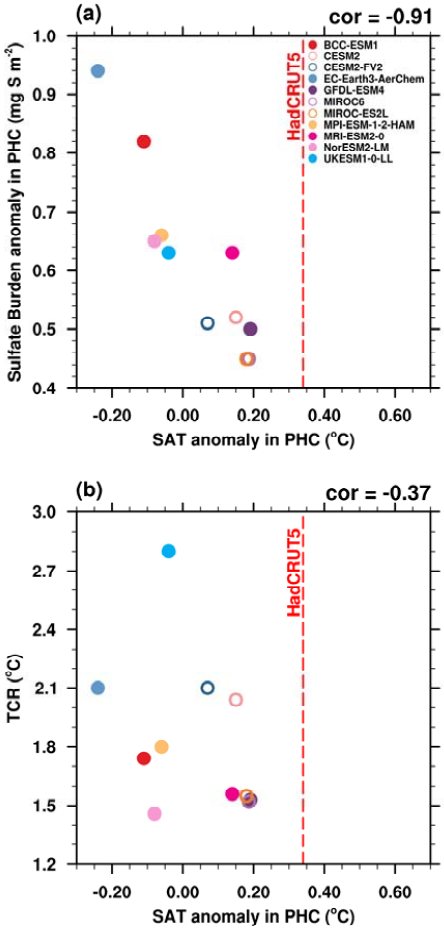

Figure 2. Scatter plots of SATa in PHC period (x-axis, °C) versus (a) sulfate burden anomaly in PHC period (y-axis, mg S m^{-2}) in historical experiments, and (b) the transient climate response (TCR, °C) for each model calculated by 1pctCO2 experiments. The corresponding correlation coefficient (COR) is shown at the top-right corner of each panel. The anomalies are relative to 1850~1900 mean. Models with and without interactive chemistry are marked by color dots and color circles, respectively.

https://doi.org/10.5194/egusphere-2025-1059
Preprint. Discussion started: 12 May 2025

Greenhouse gases (GHGs) also show a rapidly increasing trend in the PHC period. However, TCR, which can generally indicate the impact of GHGs, is insignificantly correlated with SAT anomalies in CMIP6 models and the correlation coefficient is even slightly negative (Fig.2b). Therefore, the biases of atmospheric sulfate burden and the associated sulfate aerosol cooling effects play an essential role in the anomalous-cooling biases in the CMIP6 models.

2.2 Sulfur deposition and a metric for the activity of the global sulfur cycle (ESRT)

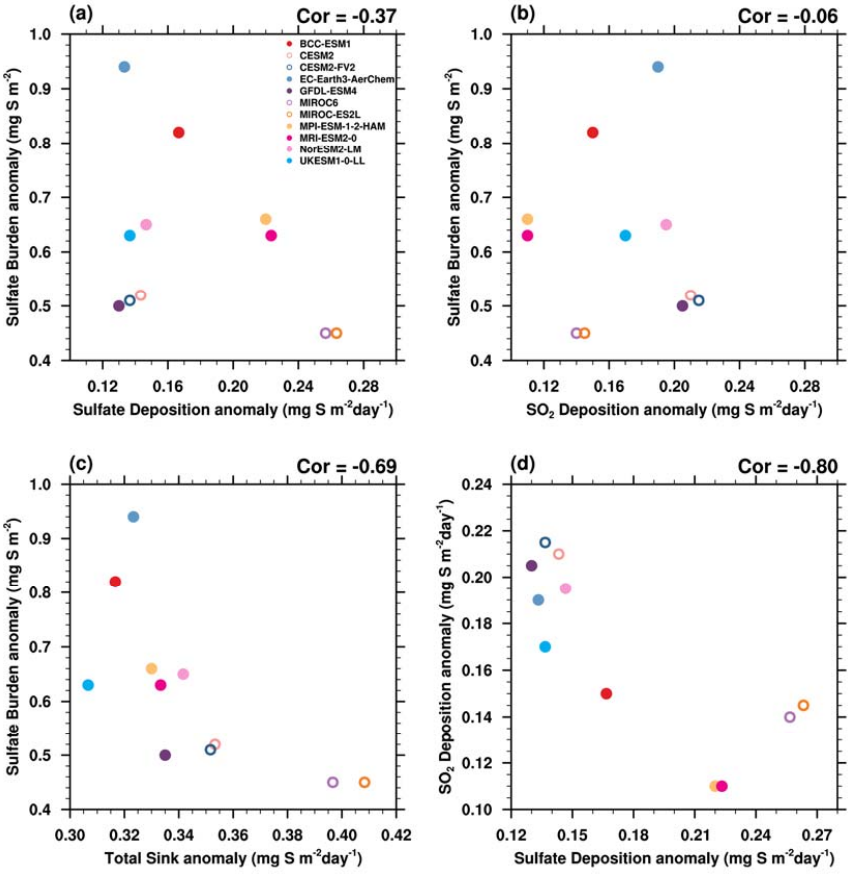

Figure 3. Sulfate burden anomaly in PHC period (mg S m^{-2}, y-axis) versus (a) sulfate deposition anomaly, (b) SO_2 deposition anomaly, and (c) total sulfur sink (sulfate and SO_2 deposition) anomaly in PHC period. (d) sulfate deposition anomaly (x-axis) versus SO_2 deposition anomaly (y-axis) in PHC period. Unit for deposition anomaly is mg S m^{-2} day^{-1}.

https://doi.org/10.5194/egusphere-2025-1059
Preprint. Discussion started: 12 May 2025

Fig. 3 shows comparisons of the global mean total sulfate burdens versus sinks of sulfur as anomalies in the PHC period relative to a baseline period of 1850~1900. As shown in Fig.3a, the sulfate burden anomaly is negatively correlated with sulfate deposition anomaly but the correlation is not significant, partly because of the presence of a group of 5 models which prevent a robust linear fitting of the remaining models by having both slow sulfate deposition rates and low sulfate concentrations. There is no clear statistical relationship between sulfate burden and SO_2 deposition (Fig. 3b). However, the correlation between sulfate burden and total sulfur sink (deposition of sulfate and SO_2) increases to -0.69, significant at the 5% level using a Student's t-test (Fig.3c). In particular, most of the 5 models with low anomalous sulfate deposition rates and low sulfate burden have higher than average SO_2 deposition, which influences their total sulfur sink enough for a correlation to emerge. We can hypothesize that in these 5 models' oxidation of precursors to sulfate proceeds slower than in the other models. This is reflected by their larger SO_2 deposition rates, and leads to less sulfate in the atmosphere. That is, both the sulfate deposition and the SO_2 deposition (via its relationship with oxidation rates) are responsible for the sulfate burden anomalies, although the relative ratio of both deposition processes is different among the models. Further examination indicates that the anomalous SO_2 deposition rate among the models is highly negatively correlated with the anomalous sulfate deposition rate with correlation coefficient of -0.80 (Fig.3d). The total sulfur sink is examined and discussed hereafter.

Considering the importance of anomalous total sulfur sink to sulfate burden, Fig.4a examines their relationship during the PHC period in each model. Generally, the anomalous sulfate burden and total sink are positively correlated and co-vary almost linearly in all the models. We further examine the ratio between sulfate burden and total sink instead of their anomalies in Fig.4b, i.e., Effective Sulfur Retention Timescale (ESRT), defined by Eq. (1) in Appendix A1. The ESRT is also approximately constant during the PHC. Comparisons indicate that the ratios between anomalous sulfate burden and anomalous total sink are highly correlated with ESRT (Fig.4c). However, the ESRT

https://doi.org/10.5194/egusphere-2025-1059
Preprint. Discussion started: 12 May 2025

is independent of preindustrial mean state and will be practically more useful. The ESRT is generally longer in models with interactive chemistry (color dot in Fig.4c) than without (color circle), which is consistent with the results demonstrated by two UK models with and without interactive chemistry (Mulcahy et al., 2020). In the two UK models sharing the same aerosol scheme, sulfate lifetime is 5.57 days in UKESM1-0-LL (which has interactive chemistry) but shorter in HadGEM3-GC3.1 (which uses prescribed concentrations for oxidants).

2.3 The recommended ESRT value

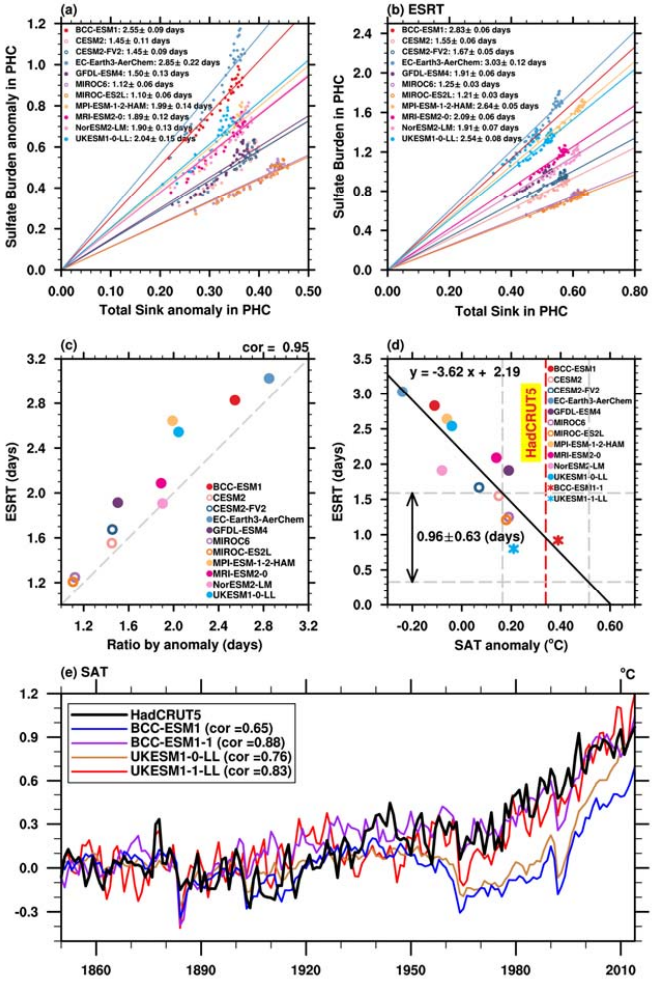

Figure 4. (a) Scatter plots of yearly total sulfur sink (*x-axis*) versus sulfate burden anomaly (*y-axis*)

https://doi.org/10.5194/egusphere-2025-1059
Preprint. Discussion started: 12 May 2025

in PHC period in relative to 1850~1900 mean. Number in legend shows the mean and standard deviation of ratio between sulfate burden anomaly and total sulfur sink anomaly in PHC period, units: days. (b) is the same as (a), but for sulfate burden and total sulfur sink. Number in legend shows the ratio defined as ESRT, units: days. (c) the ratio calculated in (a) versus ESRT in (b). (d) The SATa (ºC, x-axis) versus ESRT (days, y-axis) in PHC period for each model. The black solid line is the linear fitting. SAT anomaly in HadCRUT5 and its 0.175ºC boundaries are shown by the red solid line and parallel gray dashed lines, respectively. The constraint range for ESRT based on HadCRUT5 is 0.96±0.63 days. The red and blue asterisks are the results in the two post-CMIP6 models BCC-ESM1-1 and UKESM1-1-LL, respectively. (e) Evolutions of SAT anomalies relative to 1850~1900 mean for HadCRUT5, BCC-ESM models, and UKESM models. The numbers in legend are the corresponding correlation coefficients with HadCRUT5.

The ESRT varies from 1.21 days in MIROC6 to 3.03 days in EC-Earth3-AerChem (Fig. 4b). The standard deviation of ESRT for each model ranges from 0.03 to 0.12 days, about 3.0% of the ESRT. That is, although the sulfate burden increased significantly in the PHC period, the ESRT hardly changed. This is an important sign that ESRT is a robust index for evaluating the sulfur cycle in model development. Our finding that a single value of ESRT is capable of characterizing the anomalous cooling for each model, makes it a convenient target for model tuning. Focusing on a single, representative parameter can make tuning more efficient and help to reduce the computation cost, especially when the model resolutions become relatively high. Moreover, because ESRT has a clear physical interpretation as a globally defined efficiency factor for sulfur removal processes, tuning based on ESRT can give confidence that SAT biases are reduced for a 'right' (i.e., physically sensible) reason.

Tuning based on ESRT requires an empirical best-estimate ESRT value to aim for. Therefore, a further question is how to estimate the reasonable values for ESRT. Here we try to constrain the ESRT using the SATa in observations. Fig. 4d shows the ESRT and SATa in PHC in each model. The SATa is highly correlated with ESRT with a correlation coefficient of -0.85. The SAT anomaly in PHC is 0.34ºC, shown by the vertical red dash line (HadCRUT5). Considering the internal variability in the climate system and the uncertainty in observation, the observed uncertainty is suggested to be 0.175ºC (the vertical gray dash line parallel with the red dash line). The observed

https://doi.org/10.5194/egusphere-2025-1059
Preprint. Discussion started: 12 May 2025

uncertainty is estimated as the standard deviation of observed annual mean globally averaged SAT in HadCRUT5 from 1850 to 2014 after removing the least squares linear trend. After the constraint, the ESRT is suggested to be 0.33 to 1.59 days. As shown in the figure, most of the models have longer ESRT than expected. The ESRT in CESM2, MIROC6 and MIROC-ES2L, ranging from 1.21 to 1.55 days, is at the higher end of the suggested ESRT values, associated with their relatively low SATa. That is, the SO_2 oxidation or deposition terms in CMIP6 models may need to be modified.

Here we use this metric to modify the sulfur cycle in BCC-ESM1, more specifically we quadruple the SO_2 dry deposition over land and multiply the SO_2 dry deposition over the ocean by 1.5. This effect is similar to that in UKESM1-0-LL by modifying SO_2 dry deposition parameterization (Hardacre et al., 2021; Mulcahy et al., 2023). The impact of changes to the SO_2 dry deposition parameterization in UKESM1-0-LL is an increase of SO_2 dry deposition by a factor of 2 to 4. As shown by the red asterisk in Fig.4d, the ESRT reduced from 2.83 days to 0.92 days in updated BCC-ESM1 (BCC-ESM1-1), falling right within the recommended estimations. The new ESRT is 36% of its previous values. Accordingly, the SATa in PHC falls within the reasonable range, rising from -0.11ºC to 0.39ºC. We also examine the ESRT in UKESM1-1-LL with modified SO_2 dry deposition parameterization. The ESRT is shortened from 2.54 days to 0.80 days, also falling within the recommended ESRT range. Accordingly, the SATa in PHC period increases by about 0.25ºC. As shown by the global mean SATa in BCC-ESM and UKESM models (Fig.4e), the BCC-ESM1-1 and UKESM1-1-LL on average tracked the instrumental record quite well with higher correlation coefficients with observation. That is, in both models the improvements to the sulfur sink processes has reduced the ESRT and improved the representation of historical surface temperature observations.

3. Conclusions and discussion

Aerosol cooling effect is considered to be the second most important anthropogenic forcing over the 20th Century. Our study, based on the 11 CMIP6 models with aerosol

https://doi.org/10.5194/egusphere-2025-1059
Preprint. Discussion started: 12 May 2025

schemes, demonstrates that the anomalous cooling bias in the PHC period is closely related to the sulfate burden changes in the atmosphere. Sulfate burden in the models, and hence the strength of the anomalous cooling, is determined by sulfur deposition. We introduce a metric, called the ESRT index, which incorporates the effects of sulfur removal processes on sulfate concentration. The index is highly correlated with cooling, and can be used to constrain sulfur removal processes in models, on a global scale. In particular, we show that most models overestimate ESRT, compared to residence time-scale that would be consistent with near-zero temperature biases during the PHC period. A constraint on ESRT, derived using observed SATa, is used to inform a choice of tunable parameters for deposition in BCC-ESM1 and UKESM1-0-LL. Modifying sulfur deposition properties leads to an improved ESRT in BCC-ESM1-1 and UKESM1-1-LL, as well as SATa reproductions.

Given that CMIP6 models overestimate the cooling effects of sulfate during the PHC period, when emissions were rising, it is reasonable to assume that they will underestimate the rate of warming during periods when sulfur emissions are falling. This has potential implications for the use of CMIP6 in scenarios that incorporate clean-air measures to inform the Paris Agreement goals of limiting warming to below 2 or 1.5ºC, i.e., SSP1-2.6 and SSP1-1.9 in CMIP6 (O'neill et al., 2016). To improve the reliability of projections for such scenarios, sulfur cycle processes in models should be improved. The ESRT metric introduced in this paper provides a physically meaningful measure of the activity of the sulfur cycle, at a global scale, which we have shown can be used to improve modeled sulfur processes.

Appendix A: Methods and Data

A1 The Effective Sulfur Retention Timescale (ESRT) index

Atmospheric sulfate concentrations are determined by the emission and oxidation of sulfate precursors, as well as deposition processes. Together these processes make up the atmospheric part of the Earth's sulfur cycle. Anthropogenic SO_2 emissions are

https://doi.org/10.5194/egusphere-2025-1059
Preprint. Discussion started: 12 May 2025

the major source of sulfate aerosol over land in polluted regions. Given that the same anthropogenic SO_2 emissions are used in all the CMIP6 models, most of the differences in simulated atmospheric sulfate concentrations occur due to oxidation of SO_2 and sulfate deposition processes. Since much of the loss of SO_2 occurs locally to its emission source by oxidation and deposition, faster SO_2 deposition is associated with weaker SO_2 oxidation. Hence, for sulfate itself, the faster the sulfate deposition rate, the less the sulfate will reside in the atmosphere. That is, both the SO_2 deposition and sulfate deposition are important for the sulfate concentrations in the atmosphere, directly or indirectly.

Here we define the Effective Sulfur Retention Timescale (ESRT) index. This is calculated as the ratio between sulfate burden and sulfur deposition. The sulfur deposition combines the deposition rate of sulfate and its major precursor sulfur-dioxide gas (SO_2):

$$ESRT = loadSO4/(Dso_4+Dso_2), \quad (1),$$

where loadSO4 is total sulfate loading (i.e., the sulfate burden) in the atmosphere, Dso_4 and Dso_2 denote the total deposition (wet deposition and dry deposition) of sulfate and SO_2, respectively.

A2 The transient Climate Response (TCR) index

The transient Climate Response (TCR) index is calculated as the mean SAT anomaly of a 1pctCO2 simulation in a 20-year period centered on year-number 70, by which a doubling CO_2 concentration has occurred. It is an important metric representing CO_2-related historical warming and has been widely used for model evaluations and comparisons (Bevacqua et al., 2025; O'neill et al., 2016).

A3 CMIP6 models datasets.

Table A1. Information of the eleven CMIP6 models with aerosol schemes.

https://doi.org/10.5194/egusphere-2025-1059
Preprint. Discussion started: 12 May 2025

Model	Country	Interactive Chemistry	Members	Reference
BCC-ESM1	China	Yes	3	Wu et al., 2020; Zhang et al., 2021b
CESM2	US	No	11	Danabasoglu et al. (2020)
CESM2-FV2	US	No	3	Danabasoglu et al. (2020)
EC-Earth3-AerChem	European consortium	Yes	2	Döscher et al. (2021)
GFDL-ESM4	US	Yes	3	Dunne et al. (2020)
MIROC6	Japan	No	50	Tatebeet al. (2019)
MIROC-ES2L	Japan	No	30	Hajima et al. (2020)
MPI-ESM-1-2-HAM	Germany	Yes	3	Mauritsen et al. (2019)
MRI-ESM2-0	Japan	Yes	10	Yukimoto et al. (2019)
NorESM2-LM	Norway	Yes	3	Seland et al. (2020)
UKESM1-0-LL	UK	Yes	19	Sellar et al. (2019)

Eleven CMIP6 climate models with interactive aerosol schemes are utilized in this study, including seven models with interactive chemistry and four without (Table A1). The outputs from two CMIP6 experiments are used: (1) the historical experiment of climate change over the period 1850~2014, forced by time-varying external forcings that are based on observations of natural processes (e.g., solar activity, volcanic eruptions) and human-induced changes (e.g., greenhouse gas, aerosol emissions, land-use changes). All the available realizations for each model were used to minimize the uncertainty from internal variability in the climate system; (2) the 1pctCO2 simulations, in which CO_2 is gradually increased at a rate of 1% per year. The 1pctCO2 experiment is designed for studying model responses to CO_2 and is somewhat more realistic than rapidly increasing CO_2 such as in the abrupt-4×CO2 experiment.

Model outputs used in this study include surface air temperature (SAT) and the

https://doi.org/10.5194/egusphere-2025-1059
Preprint. Discussion started: 12 May 2025

following five sulfur-cycle variables: total atmospheric burden of sulfate (loadSO4), sulfate wet deposition and sulfate dry deposition, SO_2 wet deposition and SO_2 dry deposition. Uncertainty of the five sulfur cycle related variables is relatively smaller than SAT uncertainty among different members. For example, the standard deviation of loadSO4 in PHC among 11 CESM2 members is 4% of the interannual variability, whereas the value for SAT is about 21%. Similar results are also evident in 19 UKESM1 members, 3% for sulfate burden and 32% for SAT. Therefore, we use the first realization of historical simulations and neglect the inter-member differences for sulfur cycle related variables.

A4 HadCRUT

The monthly mean SAT from the Met Office Hadley Centre/Climatic Research Unit global surface temperature (HadCRUT) data version 5 from 1850 to 2014 is used for model evaluations (Morice et al., 2021). Considering the lack of long-term reliable observations in polar regions, we focus on SAT changes between 60ºS to 65ºN and the 'global' mean is calculated as the area-weighted mean in this latitudinal belt.

Code availability

All data processing codes are available if a request is sent to the corresponding authors.

Data availability

The HadCRUT5 dataset is accessible through Met Office Hadley Centre observations database (https://www.metoffice.gov.uk/hadobs/hadcrut5/). All the model data can be freely downloaded from the Earth System Grid Federation (ESGF) nodes (https://aims2.llnl.gov/search/cmip6/).

https://doi.org/10.5194/egusphere-2025-1059
Preprint. Discussion started: 12 May 2025

Author contributions

The main ideas were formulated by J.Z. and K.F. J.Z. wrote the original draft. The results were supervised by K.F. and S.T.T. All the authors discussed the results and contributed to the final manuscript.

Competing interests

The authors declare no competing financial and/or non-financial interests.

Acknowledgements

We acknowledge all data developers, their managers, and funding agencies for the datasets used in this study, whose work and support are essential to us.

Financial support

This work was jointly supported by the National Natural Science Foundation of China (Grant no. 42230608) and the UK–China Research and Innovation Partnership Fund through the Met Office Climate Science for Service Partnership (CSSP) China as part of the Newton Fund.

https://doi.org/10.5194/egusphere-2025-1059
Preprint. Discussion started: 12 May 2025

References

Aas, W., Mortier, A., Bowersox, V., Cherian, R., Faluvegi, G., Fagerli, H., Hand, J., Klimont, Z., Galy-Lacaux, C., Lehmann, C. M. B., Myhre, C. L., Myhre, G., Olivié, D., Sato, K., Quaas, J., Rao, P. S. P., Schulz, M., Shindell, D., Skeie, R. B., Stein, A., Takemura, T., Tsyro, S., Vet, R., and Xu, X.: Global and regional trends of atmospheric sulfur, Scientific Reports, 9, 953, 10.1038/s41598-018-37304-0, 2019.

Bevacqua, E., Schleussner, C., and Zscheischler, J.: A year above 1.5 °C signals that Earth is most probably within the 20-year period that will reach the Paris Agreement limit, Nature Climate Change, 1-4, 10.1038/s41558-025-02246-9, 2025.

Chylek, P., Folland, C., Klett, J. D., and Dubey, M. K.: CMIP5 Climate Models Overestimate Cooling by Volcanic Aerosols, Geophysical Research Letters, 47, e2020GL087047, https://doi.org/10.1029/2020GL087047, 2020.

Danabasoglu, G., Lamarque, J. F., Bacmeister, J., Bailey, D. A., DuVivier, A. K., Edwards, J., Emmons, L. K., Fasullo, J., Garcia, R., Gettelman, A., Hannay, C., Holland, M. M., Large, W. G., Lauritzen, P. H., Lawrence, D. M., Lenaerts, J. T. M., Lindsay, K., Lipscomb, W. H., Mills, M. J., Neale, R., Oleson, K. W., Otto-Bliesner, B., Phillips, A. S., Sacks, W., Tilmes, S., van Kampenhout, L., Vertenstein, M., Bertini, A., Dennis, J., Deser, C., Fischer, C., Fox-Kemper, B., Kay, J. E., Kinnison, D., Kushner, P. J., Larson, V. E., Long, M. C., Mickelson, S., Moore, J. K., Nienhouse, E., Polvani, L., Rasch, P. J., and Strand, W. G.: The Community Earth System Model Version 2 (CESM2), J. Adv. Model. Earth Syst., 12, 35, 10.1029/2019ms001916, 2020.

Dittus, A. J., Hawkins, E., Wilcox, L. J., Sutton, R. T., Smith, C. J., Andrews, M. B., and Forster, P. M.: Sensitivity of Historical Climate Simulations to Uncertain Aerosol Forcing, Geophysical Research Letters, 47, e2019GL085806, 10.1029/2019gl085806, 2020.

Döscher, R., Acosta, M., Alessandri, A., Anthoni, P., Arneth, A., Arsouze, T.,

https://doi.org/10.5194/egusphere-2025-1059
Preprint. Discussion started: 12 May 2025

Bergmann, T., Bernadello, R., Bousetta, S., Caron, L. P., Carver, G., Castrillo, M., Catalano, F., Cvijanovic, I., Davini, P., Dekker, E., Doblas-Reyes, F. J., Docquier, D., Echevarria, P., Fladrich, U., Fuentes-Franco, R., Gröger, M., v. Hardenberg, J., Hieronymus, J., Karami, M. P., Keskinen, J. P., Koenigk, T., Makkonen, R., Massonnet, F., Ménégoz, M., Miller, P. A., Moreno-Chamarro, E., Nieradzik, L., van Noije, T., Nolan, P., O'Donnell, D., Ollinaho, P., van den Oord, G., Ortega, P., Prims, O. T., Ramos, A., Reerink, T., Rousset, C., Ruprich-Robert, Y., Le Sager, P., Schmith, T., Schrödner, R., Serva, F., Sicardi, V., Sloth Madsen, M., Smith, B., Tian, T., Tourigny, E., Uotila, P., Vancoppenolle, M., Wang, S., Wårlind, D., Willén, U., Wyser, K., Yang, S., Yepes-Arbós, X., and Zhang, Q.: The EC-Earth3 Earth System Model for the Climate Model Intercomparison Project 6, Geosci. Model Dev. Discuss., 2021, 1-90, 10.5194/gmd-2020-446, 2021.

Dunne, J. P., Horowitz, L. W., Adcroft, A. J., Ginoux, P., Held, I. M., John, J. G., Krasting, J. P., Malyshev, S., Naik, V., Paulot, F., Shevliakova, E., Stock, C. A., Zadeh, N., Balaji, V., Blanton, C., Dunne, K. A., Dupuis, C., Durachta, J., Dussin, R., Gauthier, P. P. G., Griffies, S. M., Guo, H., Hallberg, R. W., Harrison, M., He, J., Hurlin, W., McHugh, C., Menzel, R., Milly, P. C. D., Nikonov, S., Paynter, D. J., Ploshay, J., Radhakrishnan, A., Rand, K., Reichl, B. G., Robinson, T., Schwarzkopf, D. M., Sentman, L. T., Underwood, S., Vahlenkamp, H., Winton, M., Wittenberg, A. T., Wyman, B., Zeng, Y., and Zhao, M.: The GFDL Earth System Model Version 4.1 (GFDL-ESM 4.1): Overall Coupled Model Description and Simulation Characteristics, J. Adv. Model. Earth Syst., 12, 10.1029/2019ms002015, 2020.

EB, U.: Protocol to Abate Acidification, Eutrophication and Ground-level Ozone, 1999.

Flynn, C. M. and Mauritsen, T.: On the climate sensitivity and historical warming evolution in recent coupled model ensembles, Atmos. Chem. Phys., 20, 7829-7842, 10.5194/acp-20-7829-2020, 2020.

Hajima, T., Watanabe, M., Yamamoto, A., Tatebe, H., Noguchi, M. A., Abe, M., Ohgaito, R., Ito, A., Yamazaki, D., Okajima, H., Ito, A., Takata, K., Ogochi, K., Watanabe, S., and Kawamiya, M.: Development of the MIROC-ES2L Earth

https://doi.org/10.5194/egusphere-2025-1059
Preprint. Discussion started: 12 May 2025

system model and the evaluation of biogeochemical processes and feedbacks, Geoscientific Model Development, 13, 2197-2244, 10.5194/gmd-13-2197-2020, 2020.

Hand, J. L., Schichtel, B. A., Malm, W. C., and Pitchford, M. L.: Particulate sulfate ion concentration and SO₂ emission trends in the United States from the early 1990s through 2010, Atmos. Chem. Phys., 12, 10353-10365, 10.5194/acp-12-10353-2012, 2012.

Hansen, J., Kharecha, P., Sato, M., Tselioudis, G., Kelly, J., Bauer, S., Ruedy, R., Jeong, E., Jin, Q., Rignot, E., Velicogna, I., Schoeberl, M., Schuckmann, K., Amponsem, J., Cao, J., Keskinen, A., Li, J., and Pokela, A.: Global Warming Has Accelerated: Are the United Nations and the Public Well-Informed?, Environment: Science and Policy for Sustainable Development, 67, 6-44, 10.1080/00139157.2025.2434494, 2025.

Hardacre, C., Mulcahy, J. P., Pope, R. J., Jones, C. G., Rumbold, S. T., Li, C., Johnson, C., and Turnock, S. T.: Evaluation of SO₂, SO₄²⁻ and an updated SO₂ dry deposition parameterization in the United Kingdom Earth System Model, Atmospheric Chemistry and Physics, 21, 18465-18497, 10.5194/acp-21-18465-2021, 2021.

Hienola, A., Partanen, A.-I., Pietikäinen, J.-P., O'Donnell, D., Korhonen, H., Matthews, H. D., and Laaksonen, A.: The impact of aerosol emissions on the 1.5 °C pathways, Environmental Research Letters, 13, 044011, 10.1088/1748-9326/aab1b2, 2018.

Hoesly, R. M., Smith, S. J., Feng, L., Klimont, Z., Janssens-Maenhout, G., Pitkanen, T., Seibert, J. J., Vu, L., Andres, R. J., Bolt, R. M., Bond, T. C., Dawidowski, L., Kholod, N., Kurokawa, J. I., Li, M., Liu, L., Lu, Z., Moura, M. C. P., O'Rourke, P. R., and Zhang, Q.: Historical (1750–2014) anthropogenic emissions of reactive gases and aerosols from the Community Emissions Data System (CEDS), Geosci. Model Dev., 11, 369-408, 10.5194/gmd-11-369-2018, 2018.

IPCC. Climate Change 2021 – The Physical Science Basis: Working Group I Contribution to the Sixth Assessment Report of the Intergovernmental Panel on

https://doi.org/10.5194/egusphere-2025-1059
Preprint. Discussion started: 12 May 2025

Climate Change, 10.1017/9781009157896, 2023.

Likens, G. E., Butler, T. J., and Buso, D. C.: Long- and short-term changes in sulfate deposition: Effects of the 1990 Clean Air Act Amendments, Biogeochemistry, 52, 1-11, 10.1023/a:1026563400336, 2001.

Mauritsen, T., Bader, J., Becker, T., Behrens, J., Bittner, M., Brokopf, R., Brovkin, V., Claussen, M., Crueger, T., Esch, M., Fast, I., Fiedler, S., Flaeschner, D., Gayler, V., Giorgetta, M., Goll, D. S., Haak, H., Hagemann, S., Hedemann, C., Hohenegger, C., Ilyina, T., Jahns, T., Jimenez-de-la-Cuesta, D., Jungclaus, J., Kleinen, T., Kloster, S., Kracher, D., Kinne, S., Kleberg, D., Lasslop, G., Kornblueh, L., Marotzke, J., Matei, D., Meraner, K., Mikolajewicz, U., Modali, K., Moebis, B., Muellner, W. A., Nabel, J. E. M. S., Nam, C. C. W., Notz, D., Nyawira, S.-S., Paulsen, H., Peters, K., Pincus, R., Pohlmann, H., Pongratz, J., Popp, M., Raddatz, T. J., Rast, S., Redler, R., Reick, C. H., Rohrschneider, T., Schemann, V., Schmidt, H., Schnur, R., Schulzweida, U., Six, K. D., Stein, L., Stemmler, I., Stevens, B., von Storch, J.-S., Tian, F., Voigt, A., Vrese, P., Wieners, K.-H., Wilkenskjeld, S., Winkler, A., and Roeckner, E.: Developments in the MPI-M Earth System Model version 1.2 (MPI-ESM1.2) and Its Response to Increasing CO2, J. Adv. Model. Earth Syst., 11, 998-1038, 10.1029/2018ms001400, 2019.

Morice, C. P., Kennedy, J. J., Rayner, N. A., Winn, J. P., Hogan, E., Killick, R. E., Dunn, R. J. H., Osborn, T. J., Jones, P. D., and Simpson, I. R.: An Updated Assessment of Near-Surface Temperature Change From 1850: The HadCRUT5 Data Set, Journal of Geophysical Research-Atmospheres, 126, 10.1029/2019jd032361, 2021.

Mulcahy, J. P., Jones, C. G., Rumbold, S. T., Kuhlbrodt, T., Dittus, A. J., Blockley, E. W., Yool, A., Walton, J., Hardacre, C., Andrews, T., Bodas-Salcedo, A., Stringer, M., de Mora, L., Harris, P., Hill, R., Kelley, D., Robertson, E., and Tang, Y.: UKESM1.1: development and evaluation of an updated configuration of the UK Earth System Model, Geosci. Model Dev., 16, 1569-1600, 10.5194/gmd-16-1569-2023, 2023.

Mulcahy, J. P., Johnson, C., Jones, C. G., Povey, A. C., Scott, C. E., Sellar, A., Turnock,

https://doi.org/10.5194/egusphere-2025-1059
Preprint. Discussion started: 12 May 2025

S. T., Woodhouse, M. T., Abraham, N. L., Andrews, M. B., Bellouin, N., Browse, J., Carslaw, K. S., Dalvi, M., Folberth, G. A., Glover, M., Grosvenor, D. P., Hardacre, C., Hill, R., Johnson, B., Jones, A., Kipling, Z., Mann, G., Mollard, J., O'Connor, F. M., Palmieri, J., Reddington, C., Rumbold, S. T., Richardson, M., Schutgens, N. A. J., Stier, P., Stringer, M., Tang, Y., Walton, J., Woodward, S., and Yool, A.: Description and evaluation of aerosol in UKESM1 and HadGEM3-GC3.1 CMIP6 historical simulations, Geoscientific Model Development, 13, 6383-6423, 10.5194/gmd-13-6383-2020, 2020.

O'Neill, B. C., Tebaldi, C., van Vuuren, D. P., Eyring, V., Friedlingstein, P., Hurtt, G., Knutti, R., Kriegler, E., Lamarque, J. F., Lowe, J., Meehl, G. A., Moss, R., Riahi, K., and Sanderson, B. M.: The Scenario Model Intercomparison Project (ScenarioMIP) for CMIP6, Geosci. Model Dev., 9, 3461-3482, 10.5194/gmd-9-3461-2016, 2016.

Ohara, T., Akimoto, H., Kurokawa, J., Horii, N., Yamaji, K., Yan, X., and Hayasaka, T.: An Asian emission inventory of anthropogenic emission sources for the period 1980-2020, Atmospheric Chemistry and Physics, 7, 4419-4444, 10.5194/acp-7-4419-2007, 2007.

Samset, B. H., Sand, M., Smith, C. J., Bauer, S. E., Forster, P. M., Fuglestvedt, J. S., Osprey, S., and Schleussner, C.-F.: Climate Impacts From a Removal of Anthropogenic Aerosol Emissions, Geophysical Research Letters, 45, 1020-1029, https://doi.org/10.1002/2017GL076079, 2018.

Seland, Ø., Bentsen, M., Olivié, D., Toniazzo, T., Gjermundsen, A., Graff, L. S., Debernard, J. B., Gupta, A. K., He, Y. C., Kirkevåg, A., Schwinger, J., Tjiputra, J., Aas, K. S., Bethke, I., Fan, Y., Griesfeller, J., Grini, A., Guo, C., Ilicak, M., Karset, I. H. H., Landgren, O., Liakka, J., Moseid, K. O., Nummelin, A., Spensberger, C., Tang, H., Zhang, Z., Heinze, C., Iversen, T., and Schulz, M.: Overview of the Norwegian Earth System Model (NorESM2) and key climate response of CMIP6 DECK, historical, and scenario simulations, Geosci. Model Dev., 13, 6165-6200, 10.5194/gmd-13-6165-2020, 2020.

Sellar, A. A., Jones, C. G., Mulcahy, J. P., Tang, Y., Yool, A., Wiltshire, A., O'Connor,

https://doi.org/10.5194/egusphere-2025-1059
Preprint. Discussion started: 12 May 2025

F. M., Stringer, M., Hill, R., Palmieri, J., Woodward, S., de Mora, L., Kuhlbrodt, T., Rumbold, S. T., Kelley, D. I., Ellis, R., Johnson, C. E., Walton, J., Abraham, N. L., Andrews, M. B., Andrews, T., Archibald, A. T., Berthou, S., Burke, E., Blockley, E., Carslaw, K., Dalvi, M., Edwards, J., Folberth, G. A., Gedney, N., Griffiths, P. T., Harper, A. B., Hendry, M. A., Hewitt, A. J., Johnson, B., Jones, A., Jones, C. D., Keeble, J., Liddicoat, S., Morgenstern, O., Parker, R. J., Predoi, V., Robertson, E., Siahaan, A., Smith, R. S., Swaminathan, R., Woodhouse, M. T., Zeng, G., and Zerroukat, M.: UKESM1: Description and Evaluation of the UK Earth System Model, J. Adv. Model. Earth Syst., 11, 4513-4558, 10.1029/2019ms001739, 2019.

Smith, C. J. and Forster, P. M.: Suppressed Late-20th Century Warming in CMIP6 Models Explained by Forcing and Feedbacks, Geophysical Research Letters, 48, 10.1029/2021gl094948, 2021.

Steffen, W., Crutzen, P. J., and McNeill, J. R.: The Anthropocene: Are humans now overwhelming the great forces of nature, Ambio, 36, 614-621, 10.1579/0044-7447(2007)36[614:taahno]2.0.co;2, 2007.

Tatebe, H., Ogura, T., Nitta, T., Komuro, Y., Ogochi, K., Takemura, T., Sudo, K., Sekiguchi, M., Abe, M., Saito, F., Chikira, M., Watanabe, S., Mori, M., Hirota, N., Kawatani, Y., Mochizuki, T., Yoshimura, K., Takata, K., O'Ishi, R., Yamazaki, D., Suzuki, T., Kurogi, M., Kataoka, T., Watanabe, M., and Kimoto, M.: Description and basic evaluation of simulated mean state, internal variability, and climate sensitivity in MIROC6, Geoscientific Model Development, 12, 2727-2765, 10.5194/gmd-12-2727-2019, 2019.

Vestreng, V., Myhre, G., Fagerli, H., Reis, S., and Tarrasón, L.: Twenty-five years of continuous sulphur dioxide emission reduction in Europe, Atmos. Chem. Phys., 7, 3663-3681, 10.5194/acp-7-3663-2007, 2007.

Wang, Z., Lin, L., Xu, Y., Che, H., Zhang, X., Zhang, H., Dong, W., Wang, C., Gui, K., and Xie, B.: Incorrect Asian aerosols affecting the attribution and projection of regional climate change in CMIP6 models, Npj Climate and Atmospheric Science, 4, 10.1038/s41612-020-00159-2, 2021.

https://doi.org/10.5194/egusphere-2025-1059
Preprint. Discussion started: 12 May 2025

Wilcox, L. J., Highwood, E. J., and Dunstone, N. J.: The influence of anthropogenic aerosol on multi-decadal variations of historical global climate, Environmental Research Letters, 8, 10.1088/1748-9326/8/2/024033, 2013.

Wu, T., Zhang, F., Zhang, J., Jie, W., Zhang, Y., Wu, F., Li, L., Yan, J., Liu, X., Lu, X., Tan, H., Zhang, L., Wang, J., and Hu, A.: Beijing Climate Center Earth System Model version 1 (BCC-ESM1): model description and evaluation of aerosol simulations, Geosci. Model Dev., 13, 977-1005, 10.5194/gmd-13-977-2020, 2020.

Yukimoto, S., Kawai, H., Koshiro, T., Oshima, N., Yoshida, K., Urakawa, S., Tsujino, H., Deushi, M., Tanaka, T., Hosaka, M., Yabu, S., Yoshimura, H., Shindo, E., Mizuta, R., Obata, A., Adachi, Y., and Ishii, M.: The Meteorological Research Institute Earth System Model Version 2.0, MRI-ESM2.0: Description and Basic Evaluation of the Physical Component, Journal of the Meteorological Society of Japan, 97, 931-965, 10.2151/jmsj.2019-051, 2019.

Zhang, J., Furtado, K., Turnock, S. T., Mulcahy, J. P., Wilcox, L. J., Booth, B. B., Sexton, D., Wu, T., Zhang, F., and Liu, Q.: The role of anthropogenic aerosols in the anomalous cooling from 1960 to 1990 in the CMIP6 Earth System Models, Atmos. Chem. Phys. Discuss., 2021, 1-39, 10.5194/acp-2021-570, 2021a.

Zhang, J., Wu, T., Zhang, F., Furtado, K., Xin, X., Shi, X., Li, J., Chu, M., Zhang, L., Liu, Q., Yan, J., Wei, M., and Ma, Q.: BCC-ESM1 Model Datasets for the CMIP6 Aerosol Chemistry Model Intercomparison Project (AerChemMIP), Advances in Atmospheric Sciences, 38, 317-328, 10.1007/s00376-020-0151-2, 2021b.